Ammonia Synthesis

James Rhodes

April 25, 2018

1 Introduction

1.1 Overview

The production process of ammonia is a key stage in converting the hydrogen gas produced in electrolysis and nitrogen from cryogenic separation of air into liquid ammonia. This is useful as it is significantly safer and cheaper to store long-term than hydrogen this is due to the significantly lower boiling point of hydrogen and thus the lower energy density of hydrogen at atmospheric conditions (2.96 MJ/L) compared to that of ammonia (13.77 MJ/L)[1] thus a not only would a volume 4.65 times greater than that of ammonia would be required for comparable energy storage. Significantly higher pressures and cryogenic temperatures would be required to store hydrogen in liquid form, making large quantities significantly more expensive to store. Stored ammonia can then be fed to the power generation side of the plant in order to match the power demand of the region, and provide long term storage for renewable wind energy without the need for the combustion of fossil fuels.

In order to produce ammonia a reversible reaction takes place between hydrogen and nitrogen. The equation of reaction for ammonia synthesis from nitrogen and hydrogen is;

$$3H_2 + N_2 \rightleftharpoons 2NH_3 \qquad \Delta h_0 = -92.44\ kJ/mol \tag{1}$$

This synthesis reaction is exothermic and can be designed in such a way that the high temperature products of reaction can be used to preheat the reactants to the operating point of reaction in an auto-thermal process. This has significant benefits in terms of reducing the energy requirements of the plant. However, the process by which the reaction takes place can vary depending on the requirements of the plant.

1.2 Design objective

The ammonia synthesis stage of the plant design was required to meet the capacity of ammonia production for the storage of excess energy produced by the wind turbines. This can subsequently be stored as liquid ammonia and be used to generate electricity in the solid oxide fuel cell and gas turbine in order to match the fluctuating electricity demand of the region. A number of different methods of ammonia synthesis have been reviewed and considered in the design process in order to design a process best suited to the scale, technology, economic constraints and environmental impact of plant.

In regard to the scale, of the process an initial year long demand requirement for stored energy was calculated in the control and energy matching design process [REFERENCE WILL] this g both a requirement for the year-long average energy demand for stored ammonia as well as the maximum energy storage requirement cause by a supply/demand deficit. These requirements are shown in table 6.2 below, using the known efficiencies of the power generation stages and their respective duties an annual demand for ammonia can be calculated. Supply-demand matching can also be used to calculate the maximum storage required throughout the year. This gives scale requirements for ammonia output and storage and thus the design requirements for my design process.

As defined by the power demand of Maui, Hawaii the year average power is set to average at a plant output of $36.6MW$. Accounting for combined generation efficiency in the ammonia-to-power stage of 61.7% this translates into a daily average ammonia output of 227.6 metric tonnes. However, this does not account for the variable supply of wind power and subsequent hydrogen. Thus the ammonia synthesis stage must be designed for a higher capacity to ensure that it can adjust to temporal fluctuations in energy supply. Thus a reactor with a capacity for 300 tonnes per day will be designed with short term hydrogen storage and an an ammonia breakdown loop to ensure continuous operation of the synthesis process.

Table 1: Design requirements of synthesis stage

Yearly output	Average output	Storage required	Power stage efficiency
83058 tonnes	227.6 tpd	15000 tonnes	61.7 %

Further considerations were given to technological requirement, whilst new and emerging

technologies were considered in the design process priority was given to methods that have been successfully implemented on medium and large scale processes, laboratory condition processes whilst considered were only chosen if there was a clear method in upscaling to industrial levels and the benefits of doing so were significantly greater than established industrial processes. This was due to the need for reliability of power supply, especially considering the island location of the power plant and the lack of alternative power sources. Finally, consideration was given to the environmental and economic considerations. These were especially important if the plant was going to have to provide clear benefits over gas and coal power generation plants. Thus the impact of waste flows was considered heavily as was the opportunities to recycle materials where possible.

2 Review of ammonia synthesis methods

2.1 Haber process

The most well established and widely used method for producing Ammonia is the process developed on an industrial scale in 1913 by Fritz Haber at BASF. This involved the reaction of N_2 and H_2 feed gases over a hetrogenous solid iron catalyst at high temperature and high pressure. The most common catalyst in this process is Fe in magnetite form. Whilst this process is well established and easily scalable with current production capacities exceeding 3000tpd [2] its low single pass conversion and large ramp-up time makes it difficult for demand matching, meaning the process is usually run as a continuous process. Despite this limitation a large number of research and improvements have been made to this process and with the addition of a recycle stream overall conversion rates above 95% are now regularly achieved. Developments into the catalyst composition used in the reactor has led to lower pressure reactors and higher single pass conversion rates.

Perhaps the most significant of these has been the development of wüstite as an alternative to magnetite as the iron precursor in the catalyst. This has shown clear advantages in terms of ammonia first pass conversion at lower temperatures and pressures and for similar material promoters[3] [4].

2.2 Ruthenium-based synthesis

A growing competitor to the iron-based synthesis route is an ammonia synthesis production route in which a Ruthenium based catalyst is used in place of the iron. Despite know usage in ammonia synthesis since 1917 it was not until 1972 that Ozaki et al demonstrated visibly higher activity in ammonia synthesis converters using Ru as an active component. This had led to field of research into its use as a catalyst and in 1992 the development of the KAAP (Kellogg Advanced Ammonia Process) industrial process for Ru-based ammonia synthesis [5]. This process is typically able to operate under significantly lower pressures and feed ratios than iron-based catalysts, meaning a clear economic advantage in terms of reactor and pressure vessel design. The tradeoff is the scarcity of Ruthenium and thus the significantly higher cost of the catalyst. This can be shown in Table 2.2 below [6].

Table 2: Comparison of ammonia synthesis catalysts

Catalyst	Availability	Cost (USD/m^3)*	T/ °C	H_2/N_2 ratio	Energy consumption (Gj/t)
Fe	abundant	4750	350-525	2-3	∼27
Ru	scarce	254100	325-450	under 2	∼27

*converted from CNY data at March 2018 exchange rates

The cost of Ruthenium being over 50 times greater than that of Iron is a huge factor in the cost of the reactor. Furthermore, the poisoning of the Ruthenium by high concentrations of hydrogen can mean the cost of replacing the catalyst.

2.3 Electrocatalysis

An alternate method of producing ammonia is to use electrocatalysis reaction. This is a non-spontaneous thermodynamic reaction:

$$3H_2O + N_2 \rightleftharpoons 2NH_3 + 1.5O_2 \qquad (K_{298} = 10^{-120}) \tag{2}$$

This can occur using electric energy. This has shown similar efficiency to established synthesis methods under normal temperatures and pressures [6]. In recent years this has been a growing field with research into materials for electro-catalysts and electrolytes. However, current

limitations of low current efficiency and conversion rates make this technology one in need of further development. Despite this the process has some clear benefits, the main one being the use of water as a hydrogen source reduces the need for hydrogen production; enabling the direct conversion of wind-generated electrical energy into ammonia.

Figure 1: Electrochemical ammonia synthesis - anode (l), cathode(r) [7]

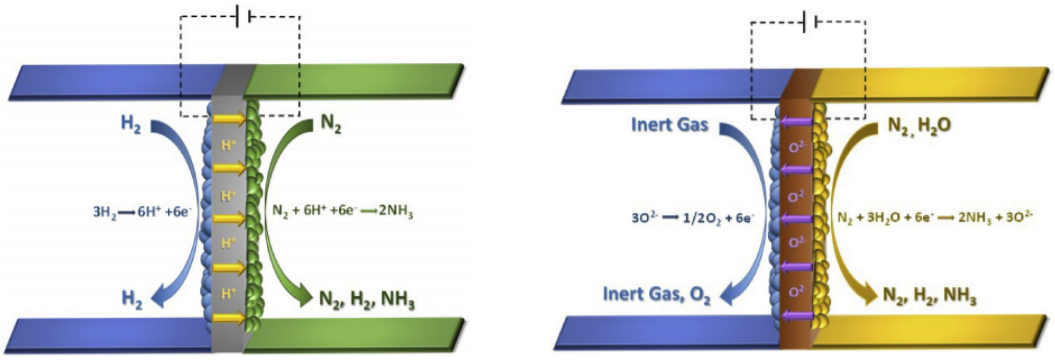

2.4 Photocatalytic synthesis

Using the same principles of photosynthesis the photocatalytic reaction of nitrogen and water to form ammonia and oxygen can be achieved at room temperature and atmospheric pressure under the addition of solar energy. However, despite ongoing research into this field and a number of photocatalysts available, the scale of this process would currently be unable to meet the ammonia requirement of the plant[6].

3 Thermodynamic modelling

3.1 Equilibrium constant

The equilibrium constant for ammonia synthesis was first calculated by Gillespie and Beattie (1930)[8] and is a function of the reaction temperature.

$$logK_a = -2.691122log(T) - 5.519265 \times 10^{-5}T + 1.848863 \times 10^{-7}T^2 + \frac{2001.6}{T} + 2.6899 \quad (3)$$

This suggests that a lower temperature produces a higher equilibrium constant, as ammonia synthesis is an exothermic reaction theory supports this result as an exothermic reversible

Figure 2: Equilibrium constant K_a of ammonia synthesis reaction at varying temperature

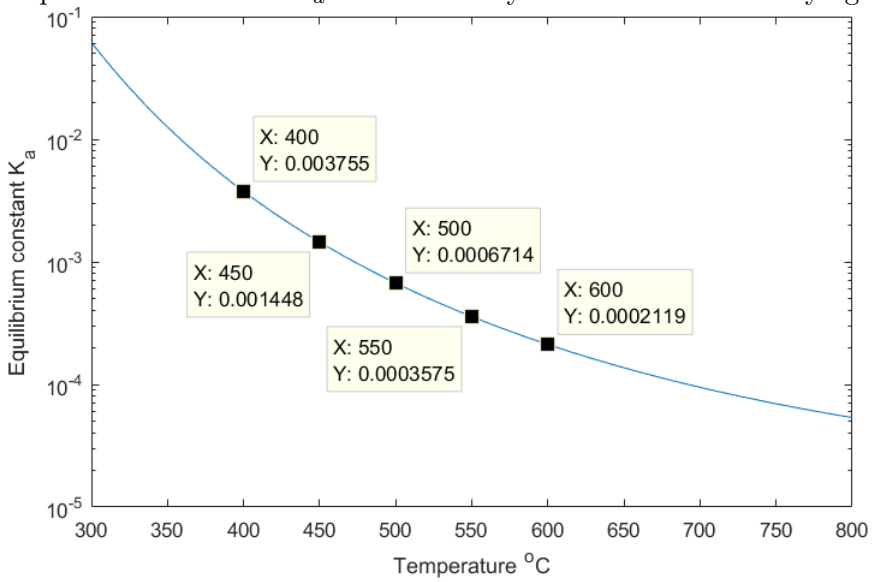

reaction favours the reactants as temperature increases.

3.2 Reaction mixtures

When calculating the properties of reaction mixtures throughout the system a rule of mixtures is used. Eqn. 4 gives the specific heat of a reaction mixture where x_i are the mole fractions in the stream and $C_{p,i}$ are their respective specific heats.

$$C_{p,mix} = x_{N_2} C_{p,N_2} + C_{p,H_2} + C_{p,NH_3} \tag{4}$$

Calculating the respective specific heats $C_{p,i}$ can be given by the polynomial temperature correlation Eqn. 5.

$$C_{p,i} = a + bT + cT^2 + dT^3 \tag{5}$$

Table 3: Specific heat coefficients [9]

Coefficient	N_2	H_2	NH_3
a	28.9	29.11	27.568
b	$-0.1571 * 10^{-2}$	$-0.1916 * 10^{-2}$	$2.5630 * 10^{-2}$
c	$0.8081 * 10^{-5}$	$10.4003 * 10^{-5}$	$0.99072 * 10^{-5}$
d	$-2.873 * 10^{-9}$	$-0.8704 * 10^{-9}$	$-6.6909 * 10^{-9}$

4 Mechanism and Kinetics

4.1 Reaction mechanism

The reaction mechanism of the ammonia synthesis stage was key in understanding the kinetics of reaction and the effectiveness of a catalyst. This is due to the need for the N_2 bond to be broken on the surface of the catalyst during adsorption but also for the need for the dissociation of the bond during the synthesis step. The established mechanism steps for the ammonia synthesis reaction is understood to be the following reaction [10].

$$H_2 + * \rightleftharpoons 2H_{ad} \tag{6a}$$

$$N_2 + * \rightleftharpoons N_{2,ad} \tag{6b}$$

$$N_{2,ad} \rightleftharpoons 2N_{ad} \tag{6c}$$

$$N_{ad} + H_{ad} \rightleftharpoons NH_{ad} \tag{6d}$$

$$NH_{ad} + H_{ad} \rightleftharpoons NH_{2,ad} \tag{6e}$$

$$N_{2,ad} + H_{ad} \rightleftharpoons NH_{3,ad} \tag{6f}$$

$$N_{3,ad} \rightleftharpoons NH_3 + * \tag{6g}$$

Where $*$ denotes the forming of an adsorption site. Experimental studies have found the adsorption of nitrogen (6b) to be the rate determining step in this process and thus leading to an understanding of the microkinetics of the rate of reaction. This is due to the strong N_2 triple bond that must be broken.

4.2 Rate of reaction

Numerous models [11] for the rate of reaction of ammonia synthesis, however, the most widely used model for the rate of reaction is the Temkin equation [12]. Whilst a number of different forms of the equation have now been developed the Dyson and Simon [13] form is preferred in this analysis due to its simplicity and the limited experimental data required to simulate results.

$$r_{NH_3} = K_2 \left[K_a^2 \times f_{N_2} \left(\frac{f_{H_2}^3}{f_{NH_3}^2} \right)^{\alpha} - \left(\frac{f_{NH_3}^2}{f_{H_2}^3} \right)^{\alpha - 1} \right] \tag{7}$$

This equation the fugacities, f, rather than partial pressures have been used. Whilst the values of the equilibrium constant K_a is well known the constant of reverse reaction K_2 and empirical constant α are found experimentally.

Figure 3: Reaction rate of ammonia synthesis

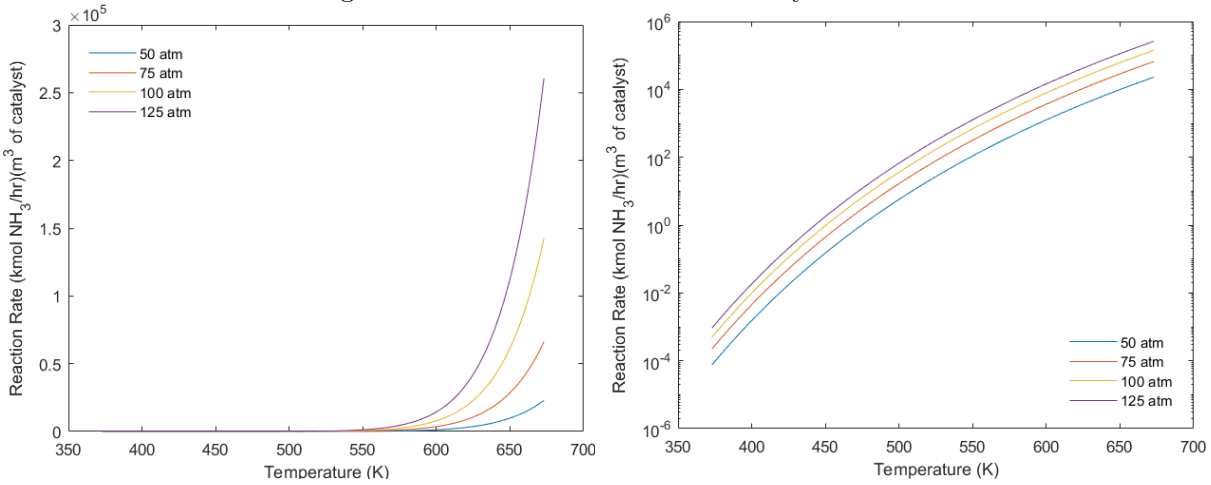

This it is clear that as temperature and pressure inside the reactor increases the rate of reaction also increases. However, whilst the rate of reaction is known to increase within the reactor the equilibrium constant of reaction moves further towards the reactants due to the exothermic nature of reaction.

Furthermore due to the NH_3 fugacities appearing in the denominator in both terms of the rate equation the equation breaks down when no ammonia is present clearly this does not follow the thermodynamic principles of a reverse reaction. Thus for the purpose of modelling a trace amount ($\leq$1%) of ammonia was included in the initial reactants. As the reactor will be run at steady state reaction is analysed.

4.3 Fugacities

The fugacities of the respective gases can be calculated using

$$f_{N2} = P\gamma_{N_2}\frac{a}{3\delta}(1 - b_2 Z) \qquad a = \frac{3\delta}{3+1}$$
$$f_{H2} = P\gamma_{H_2}a(1 - b_1 Z) \qquad b_1 = \frac{i_0+0.5+(0.5/\delta)}{1-i_0}$$
$$f_N H_3 = P\gamma_{NH_3} \times Z \qquad b_2 = \frac{i_0-0.5+1.5\delta}{1-i_0}$$

Fugacity coeffiecients γ can be calculated using the Cooper (1967) and Newton (1935) expressions given below;

$$\gamma_{N_2} = 0.93431737+0.3101804\times10^{-3}T+0.295896\times10^{-3}P-0.2707279\times10^{-6}T^2+0.4775207\times10^{-6}P^2 \tag{8}$$

$$\gamma_{H_2} = exp\{e^{(-3.8402*T^{(}0.125)+0.541)}P-e^{(-0.1263*T^{(}0.5)-15.980)}P^2+300*[e^{(-0.011901*T-5.941)}](e^{(-P/300)}-1)\} \tag{9}$$

$$\gamma_{NH_3} = 0.1438996+0.2028538\times10^{-2}T-0.4487672\times10^{-3}P-0.1142945\times10^{-5}T^2+0.2761216\times10^{-6}P^2 \tag{10}$$

The sensitivity of the fugacity coefficients to temperature can be seen on figure 4. Showing that as temperature decreases and pressure increases the behaviour of gases becomes increasingly non-ideal.

4.4 Modelling

When modelling this Kinetic model and implementing the design into ASPEN a Langmuir-Hinshelwood Hougen-Watson (LHHW) kinetic model, simulating the model using the surface mechanisms during the reactions. This is most commonly used when modelling heterogeneous reactions with a solid catalyst and fluid reactants. To simulate this model using ASPEN the general form of the model must be given [14];

$$Rate = \frac{(Kinetic factor)(Driving force)}{(Absorption)} \tag{11}$$

In this form and using the Dyson and Simon form of the Temkin equation we can set the

Figure 4: Variation of fugacity coefficients with temperature

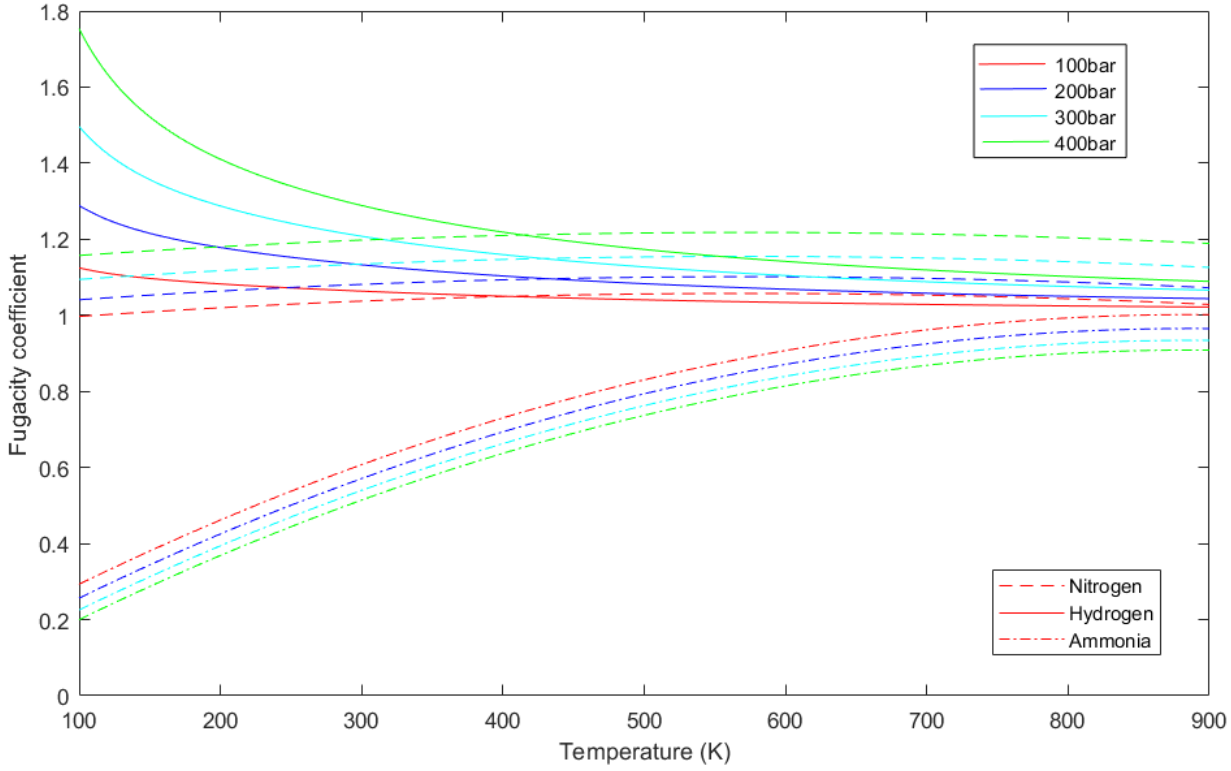

absorption term to unity and the kinetic factor to k_2, giving a driving force expression;

$$Driving force = K_a^2 \times f_{N_2} f_{H_2}^{3\alpha} f_{NH_3}^{-2\alpha} - f_{NH_3}^{(2\alpha-2)} f_{H_2}^{(3-3\alpha)} \tag{12}$$

Using the experimental values for k_20 and E^2 in the Arrhenius law to calculate k_2 and then the Gillespie and Beattie equation to calculate K_a and an experimental value of $\alpha = 0.5$ a kinetic model for the reaction was formed. Initial simulations of this model in a PFR reactor in aspen at a first approximation of industrial conditions (p=100bar T=400°C) gave an first pass conversion of $\approx 25\%$ NH_3 first pass conversion.

5 Catalyst

In modelling the rate of reaction Dyson and Simon accounted for the flow of reactants through a reactor. In order to account for the presence of a solid catalyst an effectiveness factor ξ_c was used such that an effective rate ($r_{eff} = \xi_c r_{NH_3}$) through the reactor could be calculated using the following assumptions[13]; The catalyst particles can be considered as spheres. The

diffusion coefficients of each component are independent of position within a particle, Isothermal particles, Knudsen diffusion is not experienced. Giving the equation;

$$\xi_c = \frac{\text{(molar flux of componenet i across surface)} \times \text{(surface area of catalyst pellet)}}{\text{(vol. of catalyst pellet)} \times \text{(rate of formation of component i at surface comp.,T,P)}} \quad (13)$$

Throughout the past 100 years of an Fe-based magnetite (Fe_2O_3) precursor with a variety of oxidic promoters have been the principal catalyst used industrially in ammonia synthesis [6]. However, over the past few decades a number additional catalysts have been developed. These involve the use of a various other materials as promoters including ruthenium and bimetallic nitrides, these were considered during the initial design of the plant due to their higher yields of ammonia at reduced pressures. This was mainly due to both the high cost and limited availability of Ruthenium. Considering the island location of the power generation facility the availability of resources was a key factor in the choice of catalyst.

On balance, the additional cost of these materials are substantially higher than iron and thus greatly increase both the initial capital costs of the plant but also the running costs of the plant due to the increased material costs. Thus an alternative wüstite ($Fe_{1-x}O$) iron catalyst was chosen for the ammonia synthesis stage. This was chosen due to the increased reaction rate at lower operating pressure than the traditional magnetite promoter thus reducing the pressure needed for the reactor and thus the capital costs required. The catalyst in use will be the A301 catalyst manufactured by Shangyou Catalyst Co. Ltd.

Table 4: A301 Catalyst composition

Compound	Wustite (%)
Fe oxide (Precursor)	93
Al_2O_3 (Promoter)	2.7
K_2O (Promoter)	0.8
CaO (Promoter)	2.8
Others*	0.7
*Impurities in raw material	

In the case of catalyst particles

Table 5: Wüstite catalyst properties [3]

A301 particle size	0.15-0.25mm
Bulk density	3.25 g/cm^3
BET total surface area	16.6 m^2/g
K_{20}	0.874 x 10^{16}
E_2	44.9 kcal/mol

6 Reactor design

The synthesis reactor is central to the design of the process as it is within here that the synthesis reaction takes place. In order to maintain close to optimum conditions within the reactor I have chosen to separate my reactor into two beds with intercooling between them. This enables the products of the first bed to return to a lower temperature before entering the second stage.

Figure 5: Reactor stage with integrated heat exchanger

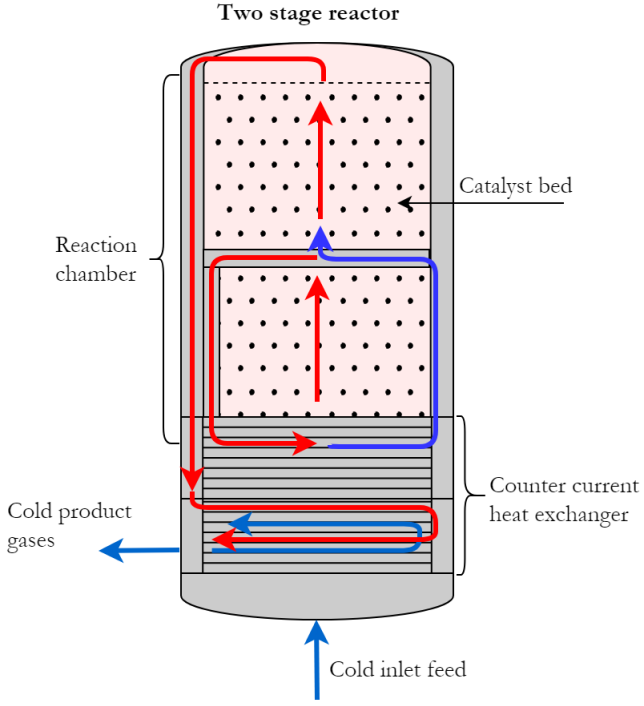

6.1 Reactor sizing

The reactor consists of two reactor stages with interstage indirect cooling. Both reactor inlet stages are designed as fixed bed reactors with an even catalyst spacing throughout. Modelling

the outlet temperature against reactor length in figure 6 for a single bed with an input temperature of 400 °C and a diameter of 0.2m shows a change in the reactor profile up to L=0.25m after this point increasing the reactor length no longer increases the NH_3 yield thus this was chosen as a suitable length for the first stage. Using this first stage design a second bed could be subsequently designed. Using a larger bed was required to optimise ammonia yield. Simulating the reactor bed on ASPEN an optimum length of D=0.25m and L=0.9m was chosen as after this point there was no significant increase in performance with reactor length, giving a first pass conversion of 35.2%.[15]

Figure 6: First and second reactor temperature and yield profile with length

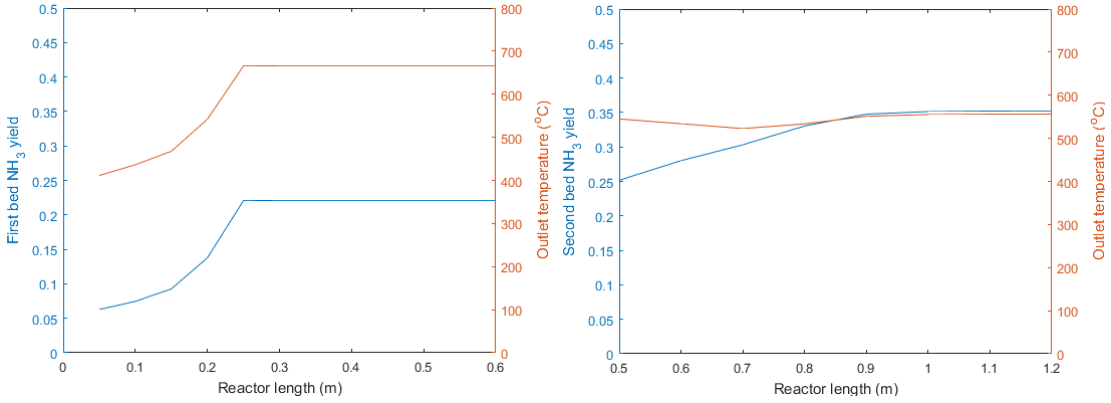

Furthermore, under a reactor pressure of 150bar the thickness of the walls must be sufficient to withstand the high internal pressures of reaction.

6.2 Material selection

In order to calculate the thickness of material required the internal reactor forces must be measured. As must the operating temperatures. From my simulation the peak temperature of normal operation of the reactor remains below 700°C. Therefore assuming a material with a melting point significantly higher than this would be required. Due to the corrosivity of NH_3 to a number of metals high-yield steel was chosen as the material for construction of the vessel.

Table 6: Properties of high yield steel [16]

Density	Melting point	Yield stress	Ultimate tensile strength	Cost
7850 kg/m^3	1500°C	400 MPa	600 MPa	$896/tonne [17]

To ensure the reactor material can withstand the reactor pressures it must both withstand the hoop and longditudinal stresses within the reactor such that.

$$\frac{\sigma_{yield}}{S.F.} \geq \sigma_L = \frac{PD}{4t} \text{ and } \frac{\sigma_{yield}}{S.F.} \geq \sigma_H = \frac{PD}{2t} \tag{14}$$

Where a safety factor of 2 is taken. This gives the condition that for high yield steel t$\geq 9.375mm$. Thus taking the thickness of the vessel is taken to be 10mm. This gives a volume of steel required of 10.75dm^3 at a combined mass of the two steel vessels to be 84.39kg without a catalyst bed present.

CHECK LEAK BEFORE BREAK CONDITION

6.3 Pressure drop

Pressure drop across a reactor can be calculated using the Ergun equation [18]

$$\frac{\Delta p}{L} = \frac{150\mu(1-\epsilon)^2}{D_p^2\epsilon^3}v_s + \frac{1.75(1-\epsilon)\rho}{D_p\epsilon^3}v_s^2 \tag{15}$$

Where Δp is the pressure drop across the length L of the bed, μ is the fluid viscosity, ϵ is the void space in the bed (taken as $\epsilon = 0.5$ [18]), ρ is the density of the fluid, D_p is the particle diameter and v_s is the superficial velocity of the fluid where $v_s = \frac{Q}{A} = \frac{\text{volumetric flow rate}}{\text{bed cross sectional area}}$.

Table 7: Reactor dimensions and pressure drop

Reactor bed	Volume (m^3)	Length (m)	Diameter (m)	Thickness (mm)	Δp (atm)
1	0.00785	0.25	0.2	10.0	
2	0.04418	0.9	0.25	10.0	

6.4 Heat exchanger

For my two stage reactor design intermediary cooling was a key factor in ensuring that the exothermic synthesis reaction did not result in an unwanted temperature increase, thus shifting the equilibrium of reaction further towards the reactants. There were two main methods considered in literature. These were direct quench cooling and heat exchanger indirect cooling.

6.4.1 Quench cooling

Direct quench cooling involves the addition of cold feed mixtures during the reactor stages in order to reduce the reactor temperature at each stage. This means that only a fraction of the total feed enters the first reactor stage.

6.4.2 Indirect cooling

Indirect cooling involved a heat exchanger passing the hot product gases past the cold feed gases in order to raise the temperature of the feed gases. This means the entire feed stream passes through all reactor stages and thus the time in the reactor is maximised.

6.4.3 Design

The chosen method for cooling configuration was the indirect cooling method due to the maximisation of reaction time. This is supported by empirical analysis [19]. The heat exchanger used in the reactor is a counter-current heat exchanger with steady state heat transfer. From this it is possible to derive an energy balance equation [20];

$$\frac{dT_c}{dx} = \frac{UA}{\dot{m}_i C_p^i L}(T_h - T_c) \tag{16}$$

$$\frac{dT_h}{dx} = \frac{UA}{\dot{m}_o C_p^o L}(T_h - T_c) \tag{17}$$

In which T_c and T_h are the respective cold inlet and hot outlet streams.A is the area for heat transfer to occur and U is the overall heat transfer coefficient of the heat exchanger ($290.35\mathrm{Wm}^{-2}K^{-1}$)[21], whilst C_p are the specific heat capacities for the respective inlet and outlet streams of gas mixtures (Eqn. 4) and $\dot{m}$ are the mass flow rates of the respective streams. Along a heat exchanger of length L where x is the relative position along it. If we then assume that assuming $\dot{m}_i c_p^i$ is equal to $\dot{m}_o c_p^o$ and similarly $\frac{UA}{\dot{m}_i c_p^i}$ does not depend on x. Then we can simplify the above expressions in order to give the temperature at the reactor inlet;

$$T_r^i = \frac{T_i + \frac{UA}{\dot{m}_i C_p^i} T_r^o}{1 + \frac{UA}{\dot{m}_i C_p^i}} \tag{18}$$

Similarly for the outlet of the heat exchanger

$$T_o = \frac{T_r^o + \frac{UA}{\dot{m}_i C_p^i} T_i}{1 + \frac{UA}{\dot{m}_i C_p^i}} \tag{19}$$

The aim of the heat exchanger is twofold. The first of these is to heat up the feed of the product gases to a significantly high temperature to allow for a suitable rate of reaction. This is done by running the hot product gases in counter current to the feed gases. The second use of the heat exchanger is in a two-stage reactor system the heat exchanger acts as an intermediary coolant for the product gases. This brings the temperature down to one in which the reaction equilibrium maintains a increased fraction of ammonia products.

7 Additional units

7.1 Separator

In order to remove the fraction of ammonia from the product mixture the relatively high boiling point of ammonia was used to remove liquid ammonia at high pressure and low temperature in a separator. This separates liquid droplets from gas particles by using gravity separation to allow the gaseous products to leave from the top outlet whilst liquid ammonia is removed from the bottom outlet in a vertical separator.

To separate liquid ammonia from the product gases I have used the Souders-Brown design equations to equate the drag force F_D exerted by gas flow to the gravity force of the droplet weight F_G [22] [23]. Such that assuming plug flow $F_D = F_G$. Substitution of expressions for the forces on a spherical droplet give the Souders-Brown expression [24];

$$V_{Gmax} = K_s \sqrt{\left(\frac{\rho_L - \rho_G}{\rho_G}\right)} \; when \; K_s = \sqrt{\left(\frac{4gD_P}{3C_D}\right)} \tag{20}$$

$$D_{min} = \sqrt{\left(\frac{(4/\pi)q_a}{F_G V_G max}\right)} \tag{21}$$

Where K_s is found experimentally. Using a high mist extractor - a horizontal wire mesh pad in a vertical separator used to coalesce the liquid into droplets large enough to drop from the

mesh pad gives $K_s = 0.12$. For a length/diameter ratio of 3/1 to reduce the material required in construction. And using a industrial standard XXX steel the separator can be modelled as a thin walled pressure vessel to calculate the required wall thickness of the tank.

$$\sigma_{yield} = \frac{pr}{t} \tag{22}$$

For an internal pressure of 140bar, known material and dimensions the separator can be sized.

Figure 7: Vertical separator with mist extractor

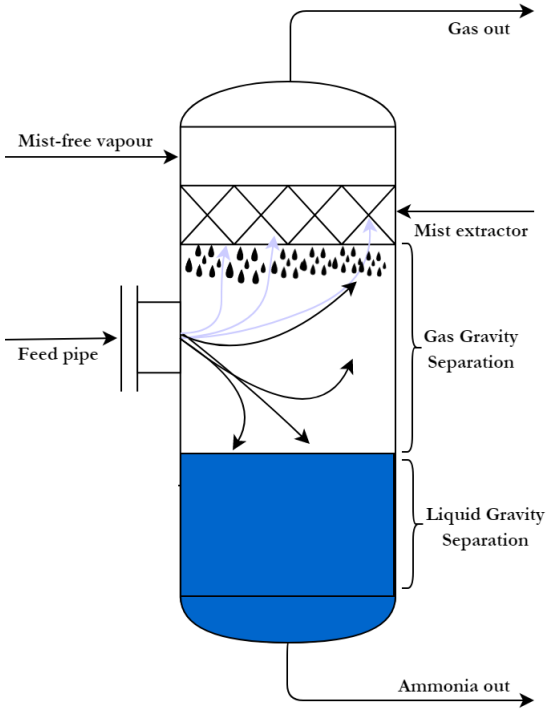

7.2 Compressor

In order to obtain the high operating pressures required for ammonia synthesis centrifugal compressors are used both in the feed streams and in the reactor inlet stream. The feed stream is used to raise the pressure of the new feed to the pressure of the recycle stream whilst the reactor inlet the stream the recycle/feed mix is compressed to raise the pressure to account for the pressure drop of reaction. In this analysis we can assume that the compressors are driven by electric motors, however, turbine powered compressors are also possible; had the gas turbine generator been run continuously for power generation this would also have been considered. For

an isentropic compressor the total output temperature can be calculated from Eqn. 23 [9].

$$T_{out} = T_{in}\left[\left(\frac{P_2}{P_1}\right)^{\frac{1}{N}}\right]^{\left(\frac{n-1}{n}\right)} \tag{23}$$

The total compression power required $\dot{W}_{fluid}$ for the fluid is given by Eqn. 24

$$\dot{W}_{comp} = \frac{\dot{W}_{fluid}}{\eta_{comp}} = \frac{1}{\eta_{comp}} TN \frac{n}{n-1} R\dot{m}\left(\left[\left(\frac{P_2}{P_1}\right)^{\frac{1}{N}}\right]^{\left(\frac{n-1}{n}\right)} - 1\right) \tag{24}$$

Where T is the input temperature, N is the number of compressor stages, n is the polytropic exponent, R the specific gas constant, $\dot{m}$ is the mass flow rate and P_1 and P_2 are the respective inlet and outlet pressures. η_{comp} is the overall compressor efficiency which the product of mechanical and isentropic efficiencies such that $\eta_{comp} = \eta_{is}\eta_m$. Standard efficiences of centrifugal compressors are taken as $\eta is = 0.85$ and $\eta_m = 0.95$ REFERENCE HERE.

7.3 Purge

In order to limit the build up of inert gases within the synthesis loop a fraction of the recycle loop is purged. However, due to the cost of obtaining feed gases it is beneficial to keep the purge fraction small. After simulating a number of purge fractions on ASPEN a fraction of 5% of the recycle stream was chosen. This purge stream is comprised of mostly H_2 and N_2 feed gases. Considering the high energy requirement of the electrolyser hydrogen recovery of this stream is in both environmental and economic interest. For this stage there are two main methods; membrane technology and cryogenic separation. With the former generally requiring a lower initial investment whilst the latter provides a greater energy efficiency [25]. In the initial

In order to fu

8 Optimising operation and control

8.1 ASPEN simulation

8.2 Plant control

9 Ammonia storage

Storage of liquid ammonia product the main method in which the supply and demand sides of the plant are matched. Thus the scale of this storage must be one of the largest stores in the plant. Liquid ammonia has a boiling point of -33.3°C at atmospheric conditions, however, this can be increased by pressure storage. This requires a compromise to me made between low temperatures and high pressures in which to store ammonia. A review of current large-scale ammonia storage methods (Bartels,2008)[1] with the main trade-off between high pressure and low temperature storage being the high capital cost of building high pressure vessels against the increased energy requirements and thus running costs of maintaining low temperature storage.

9.1 High pressure storage

Does not loose any required fuel, does not require energy to maintain. Limited by material used for the pressure vessel. So to increase capacity more vessels would be required. Bartels calculates that to store ammonia at an ambient temperature of 20^oC a pressure of 8.58 bar would need to be maintained. However, the limiting size of a steel pressure vessel is calculated to be approximately 270t. The recommended ratio is about 2.8ton NH_3 stored for every tonne of steel.

9.2 Low temperature storage

Storage a of NH_3 at low temperature and ambient pressure is commonly used for large scale storage due to higher ammonia/steel ratio and thus a reduction in capital cost. At atmospheric pressure approximately 43 tonnes of ammonia can be stored per tonne of steel. This massively reduces the capital cost on steel. Despite this other factors must also be considered, the main on being the boil-off rate of liquid ammonia due to heat transfer from the environment. This is typically below a conservative estimate of 0.1% per day [26]. This can then be captured and re-condensed at a total efficiency of 93.6% [INSERT SOURCE] using an ammonia refrigeration cycle system For a 15000 tonnes of ammonia storage a storage tank of at least 21.997×10^3 m^3 would be required (density of liquid ammonia, $\rho_{NH_3(l)}$=681.9 kg/m^3)[27].

Figure 8: Cold NH_3 storage cycle

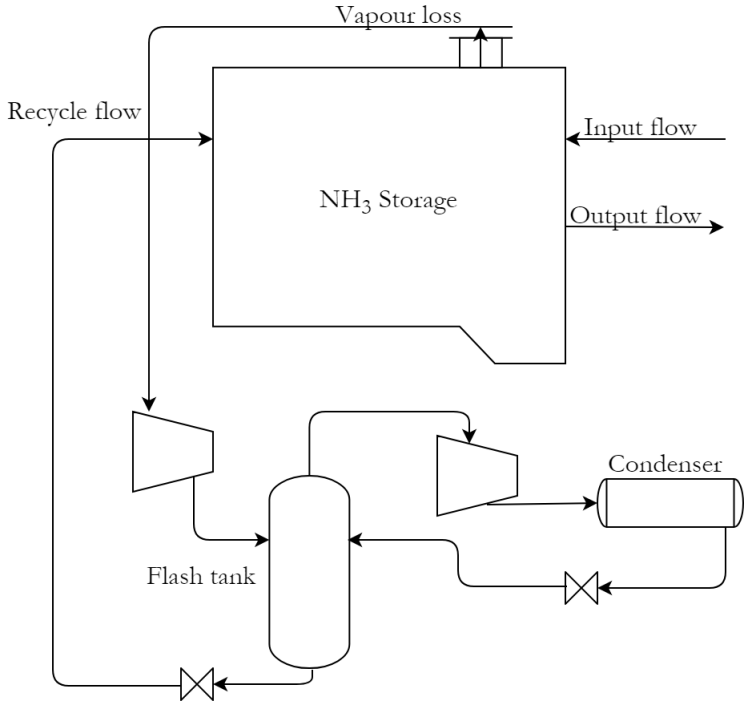

9.3 Design

As calculated in [REFERENCE THE DEMAND/SUPPLY PROFILING] the maximum capacity for required ammonia storage is calculated to be 15000 tonnes at maximum capacity. Due to the scale of the process this would require at least 55 pressure vessels with over 5000 tonnes of steel.

Table 8: Ammonia storage methods

Ammonia Storage - 15000 tonnes required		
Properties	High pressure	Low temperature
NH_3 Energy density (MJ/L)	13.77	15.37
Ammonia/Steel ratio	2.8	43
Pressure required (bar)	8.58	Atmospheric
Temperature required (^{o}C)	20	-33.3
Storage efficiency	100%	96.3%
Tanks required	55	1
Steel required (tonnes)	5357	349
Capital cost* ($ m)	4.800	0.3127

*Cost of steel at $896/tonne [17]

In order to minimise the heat transfer we want to minimise the surface area/volume ratio of the storage tank, however, despite the optimal ratio of a cylindrical tank the 3d nature of the shape would cause significant structural issues in building a sufficiently large container, thus a 3d projection of a 2 dimensional shape is preferred in order to maintain vertical structural supports. The optimal shape of this design is a cylindrical storage tank. For a maximum volume of 21.997×10^3 m^3 the optimum radius/height ratio is $\frac{h}{r} = 2$ giving a radius, r = 15.184m and height, h = 30.38m steel containers.

Estimating the hydrostatic pressure at the bottom of the storage container can be given by the equation;

$$P_h = \rho g h \tag{25}$$

In the case of ammonia the pressure on the bottom of the tank would be 203.144 MPa of additional pressure. This a suitable steel thickness would have to be chosen to withstand this.

10 Ammonia cracker

In order to produce feed gases for the gas turbine the liquid ammonia must first be decomposed into N_2 and H_2 in the endothermic reaction [28].

$$2NH_3 \rightleftharpoons 3H_2 + N_2 \qquad \Delta h_0 = 46kJ/mol \tag{26}$$

This requires the addition of heat due to the endothermic nature of the reaction and thus must be conducted in a furnace with a nickel catalyst to achieve the conversions required to decomposition.

Figure 9: Ammonia cracker flow network

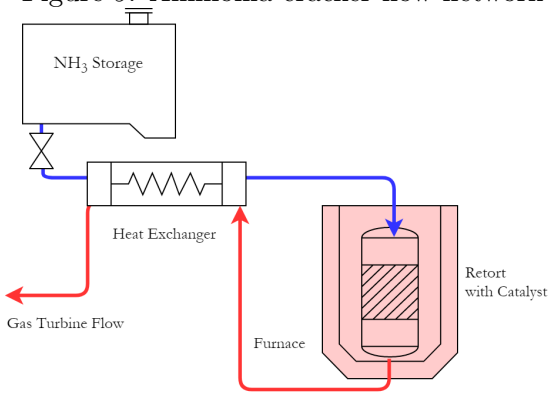

Due to the high peak demands of the 3 gas turbines a small amount of storage of the cracked gas is stored in order to ensure there is sufficient capacity to meet short term spikes. This is 300 times less than the capacity of the ammonia storage tank. This is done to reduce the capacity requirement of the cracker. The standard capacity of a industrial cracker is 1000 m^3/h at operating conditions the plant would require 26 SINCE-GAS ANH units at a cost of $6000 per unit [29].

Table 9: Ammonia cracker design requirements

Peak NH_3 mass flow demand	32.815 kg/s
Average NH_3 mass flow rate required	0.1648 kg/s
Ramp-up time of SOFC	0.5h
Maximum theoretical capacity required	59067 kg/SOFC ramp-up
Minimum turbine down-time	2h
Capacity requirement of cracker	5.469 kg/s
Cracked gas storage requirement	49.223 ton
Total cost of cracker	$156,000

11 Safety and environmental assessment

Ammonia synthesis and power generation plants possess a large number of risks associated with them, both in term of their operating conditions but also due to the chemical risks of the materials stored within the plant.

A recent history has shown that over the past 50 years whilst the rate fires within an ammonia synthesis plant has decreased over time, it remains nontheless a major risk [25][30].

A number of studies and risk reviews have been conducted over the past 50 years on the operation and source of risks and failure within Ammonia synthesis plants. In INSERT SOURCE the individual process components are analysed and the major risks are identified for causing serious incident.

11.1 Chemical risk and hazards

Easily the two most high risk elements of the process are associated with hydrogen and ammonia storage and synthesis. This is due to both the conditions of the process and the chemical effects of the compounds.

In the case of hydrogen, the main risk associate with it is in storage of high quantities of compressed gas. This is due to the risk of explosion of hydrogen gas under high temperature and pressure. The first method in which to manage this risk is through pressure relief valves in to prevent overpressurization and allow the release of gases before fracture of the storage vessel. However, whilst this prevents the overpressurization within the storage vessels, the formation of hydrogen gas clouds can become present in certain atmospheric conditions and this adequate monitoring of any valve flow must be made and subsequent ventilation of the outlet gas.

Ammonia has a number of chemical effects whilst it is not considered a flammable hazardous product due to its high autoignition temperature (651 °C) and a explosive limit of 16-25% SOURCE HERE, the first of these being its corrosivity to many metals and alloys including copper and zinc, this means that any storage, piping or fittings to come into contact with ammonia should be made only from Iron and Steel as these do not suffer from the corrosivity on contact of other metals.

Despite its lower density than air evidence suggests that the formation of ammonia gas clouds at ground level is possible in certain environmental conditions [31]. These are largely dependent on wind speed and humidity. Furthermore, despite the possibility of large ammonia clouds forming after a matter of hours the airborne ammonia concentration can change significantly, giving a poor indication of the concentration during the initial release [SOURCE].

The impact of such releases can be varied, and the number of fatalities does not appear to correlate strongly to the amount of ammonia released. A 1400 ton release of ammonia in Lithuania (1989), the largest ever recorded, resulted in a 400km2 affected area and a fatality rate of 7 people, whilst a 38 ton release of ammonia in South Africa (1973) resulted in 18 fatalities, the highest recorded involving ammonia. This was due to the proximity of a urban population, the speed of ammonia release - caused by brittle fracture - and the environmental conditions at the time - low wind in the direction of the human population.

Gaseous ammonia can cause severe irritation to the eyes, nose throat and lungs at high enough

concentrations whilst contact with liquid ammonia can cause cryogenic burns. The main hazards associated with the levels of toxicity of ammonia and the associated levels of ammonia associated with each hazard is presented in a table below.

Table 10: SOURCE

Hazard	Concentration (PPM)
Threshold limit value (TLV)	25
Short term exposure limit (STEL)	35
Immediately dangerous to life and health (IDLH)	300
Severe eye and respiratory irritation. Permanent damage	400-700
Convulsive coughing and bronchial spasms	1700
Life threatening	2500
Death from suffocation	5000-10000

Further information on the impact of exposure to ammonia can be found in the Acute Exposure Guideline Levels (AEGS) [32].

When considering methods in which to minimise the hazards caused by ammonia release into the surroundings, a number of methods are available to reduce the risk of a the formation of a high concentration release of ammonia cloud forming. The first of these is the location of the discharge valve. If positioned sufficiently high above ground level the distance travelled to ground level is sufficiently far to allow any high concentrations releases of ammonia to dilute before it reaches the ground, preventing a cloud at ground level forming. Furthermore, the installation of a mist extractor prevents liquid droplets of ammonia being released into the atmosphere. This is especially important due to the highly toxic nature of ammonia on water ecosystems, as was the case in Arkansas, USA (1971) when a 600 ton spill resulted in the death of thousands of fish on contact with a watercourse, despite no human fatalities [25].

Whilst a number of methods of managing ammonia and hydrogen release into the atmosphere have been mentioned, the most effective way of minimising the risks associated with ammonia and hydrogen gas is to limit the amount released by normal operation of the plant. This is done by recycling both the purge stream and the vented gas stream from cold storage ammonia. This is done by a reliquification feedback loop.

In the case of the purge a membrane unit under a pressure gradient is used to separate the hydrogen from the purge so that it can be recovered and added back into the hydrogen feed. In the ammonia vented case it is passed through a flash tank and condenser before being re added to the liquid ammonia tank.

In regard to the location of the ammonia storage tank, it must be placed outside of any plant buildings and at away from any densely populated urban areas and clear of any combustible materials. Furthermore, the storage tank will be at least 100m from any open water storage tank or source of potable water. And any storage location must be easily accessible by road to emergency vehicles and personnel. During any time at which the site is unattended constant monitoring of all liquid and vapour levels must take place whilst any valves with the exception of emergency pressure relief valves must be capped.

Table 11: HAZOP analysis of synthesis stage

Line	Deviation	Cause	Consequences	Action
Reactor	No	Valve stuck/blocked	Rapid temperature change, Catalyst damage, Reaction rate fall.	Measure temperature with a thermocouple and flow rate continuously with alarm and shut down system, catalytic testing.
	Less	Low output concentration, Reactor leakage, Temperature fall	Release of reactants, fall in output	Measure concentrations of gases outside of the reactor to detect any leakage of reactants. Catalyst replacement.
	More	Overpressure Overtemperature	Vessel failure, release of reactor gases.	Pressure and temperature sensors and warnings, complete shutdown at system before critical level reached. Alarm system in place.
Heat Exchanger	No	Valve stuck, blockage	Pipe burst - gas leak	Flow path redundancy in HX.
	Less	Low heat exchange - damage to surface plate, low flow rate.	Fall in output, damage to HX.	Thermocouple to measure temperature profile of flow. Regular maintenance.
	More	High flow rate, high temperature	Overheating of reactor.	Measure flow temperature. Regular maintenance.
Compressor	No	No flow - pump blockage, no power supply, complete pressure loss - leak of compressor	Gas leak into atmosphere, reduction in reaction conversion	Gas monitoring outside chamber, regular maintenance.
	Less	Low compression level - low power supply/blockage in system	Inefficient operation, damage to pump.	Filter of feed, flow rate and pressure monitoring.
	More	Overcompression, power surge, control failure, high flow rate	Damage to compressor pump, pipe rupture.	Power buffer systems. Warning and detection alarms.
Separator	No	No output flow - separator leak	No ammonia output, gas leak	Continuous monitoring of pressure, temperature and flow rates. Regular inspection.
	Less	Temperature too high	Mesh damage, low yield.	Regular stream testing. Periodic inspection.
	More	Temperature too low	Power wastage in cooling.	Thermocouple to measure vessel temperature.
Storage	No	No	Failure power generation stages	Monitoring of storage levels, low storage warning.
	Less	Refrigeration failure of vessel	Building up of pressure - burst vessel	Leak before burst design of storage tank. Pressure relief valve.
	More	Buildup of pressure in container - failure of gas release valve	Vessel failure/bursting	Redundancy in release valves, regular inspection. Pressure monitoring inside vessel.

12 Economic assessment

An economic analysis of the requires an assessment of the costs associated with each stage of the design.

13 Results and process summary

During the final design iteration of the synthesis stage a first pass conversion rate of 28% can be achieved after optimization. This is achieved at a pressure of 150bar and a reactor inlet temperature of 400°C. Figure 10 shows the final stage ammonia synthesis stage ASPEN flow diagram.

Figure 10: ASPEN model of synthesis reaction

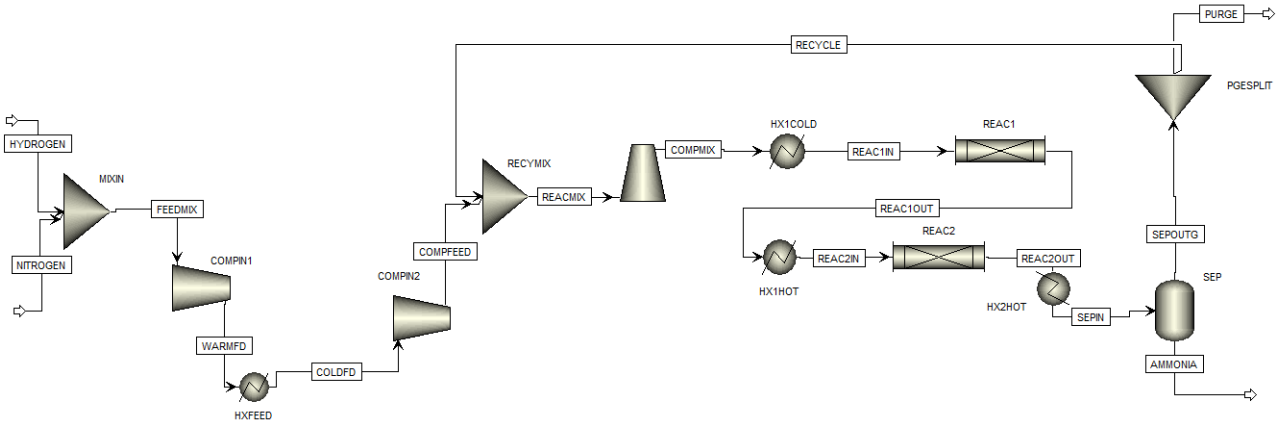

The ammonia synthesis, whilst a well established process requires careful design and optimisation of the process due to the specific design requirements. The use of ASPEN and MATLAB has allowed for the creation of a dynamic modelling system that has enabled the conversion rate of ammonia within the reactor to be optimised, whilst design of the ammonia storage requirements and power generation needs of the plant have enabled the output of this stage to be designed to minimise the waste output of the plant through stream recycles.

References

[1] Jeffrey R Bartels. A feasibility study of implementing an Ammonia Economy. *Digital Repository @ Iowa State University*, (December):102, 2008.

[2] René Bañares-alcántara and Maurizio Fiaschetti. Analysis of Islanded Ammonia-based Energy Storage Systems. (October):1–150, 2014.

[3] N. Pernicone, F. Ferrero, I. Rossetti, L. Forni, P. Canton, P. Riello, G. Fagherazzi, M. Signoretto, and F. Pinna. Wustite as a new precursor of industrial ammonia synthesis catalysts. *Applied Catalysis A: General*, 251(1):121–129, 2003.

[4] H. Z. Liu, X. N. Li, and Z. N. Hu. Development of novel low temperature and low pressure ammonia synthesis catalyst. *Applied Catalysis A: General*, 142(2):209–222, 1996.

[5] Ilenia Rossetti, Nicola Pernicone, Francesco Ferrero, and Lucio Forni. Kinetic study of ammonia synthesis on a promoted Ru/C catalyst. *Industrial and Engineering Chemistry Research*, 45(12):4150–4155, 2006.

[6] Huazhang Liu. Ammonia synthesis catalyst 100 years: Practice, enlightenment and challenge. *Cuihua Xuebao/Chinese Journal of Catalysis*, 35(10):1619–1640, 2014.

[7] V. Kyriakou, I. Garagounis, E. Vasileiou, A. Vourros, and M. Stoukides. Progress in the Electrochemical Synthesis of Ammonia. *Catalysis Today*, 286:2–13, 2017.

[8] Louis J. Gillespie and James A. Beattie. The thermodynamic treatment of chemical equilibria in systems composed of real gases. III. Mass action effects. The optimum hydrogen: Nitrogen ratio for ammonia formation in the haber equilibrium. *Journal of the American Chemical Society*, 52(11):4239–4246, 1930.

[9] Eric R Morgan. Techno-Economic Feasibility Study of Ammonia Plants Powered by Offshore Wind. *University of Massachusetts - Amherst, PhD Dissertations*, page 432, 2013.

[10] J. R. Jennings. Catalytic Ammonia Synthesis. Fundamentals and Practice. *Springer Science & Business Media*, page 451, 1991.

[11] Luis M. Aparicio and James A. Dumesic. Haber Bosch overall + conversion. *Ammonium Nitrate Project*, 1(9):452, 2008.

[12] U. Guacci, F. Traina, G. Buzzi Ferrarla, and R. Barisone. On the Application of the Temkin Equation in the Evaluation of Catalysts for the Ammonia Synthesis. *Industrial and Engineering Chemistry Process Design and Development*, 16(2):166–176, 1977.

[13] D. C. Dyson and J. M. Simon. A kinetic expression with diffusion correction for ammonia synthesis on industrial catalyst. *Industrial and Engineering Chemistry Fundamentals*, 7(4):605–610, 1968.

[14] Aspen Plus. Aspen Plus Ammonia Model. 2008.

[15] S. S.E.H. Elnashaie. Response To Comments On Simulation and Optimization of an Industrial Ammonia Reactor. *Industrial and Engineering Chemistry Research*, 28(8):1267, 1989.

[16] A. M. Howatson, P. G. Lund, and J. D. Todd. Engineering Tables and Data. 1972.

[17] Meps. Regional Steel Prices & Indices Country Steel Prices Steel Data / Statistics. pages 1–2, 2018.

[18] Sabri Ergun and A. A. Orning. Fluid Flow through Randomly Packed Columns and Fluidized Beds. *Industrial & Engineering Chemistry*, 41(6):1179–1184, 1949.

[19] Mathias Penkuhn and George Tsatsaronis. Comparison of different ammonia synthesis loop configurations with the aid of advanced exergy analysis. *Energy*, 137:854–864, 2017.

[20] Asanthi Jinasena, Bernt Lie, and Bjørn Glemmestad. Dynamic Model of an Ammonia Synthesis Reactor Based on Open Information. *9th EUROSIM Congress on Modelling and Simulation Oulu*, pages 943–948, 2016.

[21] S. S E H Elnashaie, A. T. Mahfouz, and S. S. Elshishini. Digital simulation of an industrial ammonia reactor. *Chemical Engineering and Processing*, 23(3):165–177, 1988.

[22] John M. Campbell. Gas-Liquid Separators Sizing Parameter. (December 2014):1–16, 2015.

[23] Todd B. Jekel, Douglas T. Reindl, and J. Michael Fisher. Gravity Separator Fundamentals and Design. *Ammonia Refrigeration Convention & Exhibition*, (1998):23, 2001.

[24] Mott Souders and George Granger Brown. Design of Fractionating Columns: I. Entrainment and Capacity. *Industrial and Engineering Chemistry*, 26(1):98–103, 1934.

[25] Madhusoodan Ojha and A K Dhiman. Problem , Failure and Safety Analysis of Ammonia Plant : a Review. *International Review of Chemical Engineering*, 2(October):631–646, 2010.

[26] V.C Belapurkar. Boil-Off in Refrigerated Ammonia Tanks Boil-Off in Refrigerated Ammonia Tanks. pages 1–4, 2016.

[27] V Hacker, V Hacker, K Kordesch, K Kordesch, Wolf Vielstich, Wolf Vielstich, Arnold Lamm, Arnold Lamm, Hubert a Gasteiger, and Hubert a Gasteiger. Ammonia crackers. *Facilities*, 3:121–127, 2003.

[28] J. H. Kim, D. H. Um, and O. C. Kwon. Hydrogen production from burning and reforming of ammonia in a microreforming system. *Energy Conversion and Management*, 56:184–191, 2012.

[29] Since Gas. Automatic Ammonia Cracker for Hydrogen Generation , 5-1000Nm3/h Capacity. pages 4–6, 2018.

[30] Gerald P. Williams. Safety performance in ammonia plants: Survey VI. *Process Safety Progress*, 18(2):78–81, 1999.

[31] R. F. Griffiths and G. D. Kaiser. Production of dense gas mixtures from ammonia releases - A review. *Journal of Hazardous Materials*, 6(1-2):197–212, 1982.

[32] Robert A Michaels and R A M Trag Corp. Emergency Planning : Critical Evaluation of AEGLs for Ammonia. 17(2):179–184, 1998.